NeuroImage: Clinical 13 (2017) 24–32

Contents lists available at ScienceDirect

NeuroImage: Clinical

journal homepage: www.elsevier.com/locate/ynicl

Resting-state theta band connectivity and graph analysis in generalized social anxiety disorder

Mengqi Xing[a,1], Reza Tadayonnejad[b,1], Annmarie MacNamara[b], Olusola Ajilore[b], Julia DiGangi[b], K. Luan Phan[b,c,d,e], Alex Leow[a,b], Heide Klumpp[b,c,*]

[a] Department of Bioengineering, University of Illinois at Chicago, Chicago, IL, United States
[b] Department of Psychiatry, University of Illinois at Chicago, Chicago, IL, United States
[c] Department of Psychology, University of Illinois at Chicago, Chicago, IL, United States
[d] Department of Anatomy and Cell Biology, University of Illinois at Chicago, Chicago, IL, United States
[e] Mental Health Service Line, Jesse Brown VA Medical Center, Chicago, IL, United States

ARTICLE INFO

Article history:
Received 5 August 2016
Received in revised form 29 October 2016
Accepted 11 November 2016
Available online 12 November 2016

Keywords:
EEG
Connectomics
Graph theory
Social anxiety disorders
Major depressive disorder

ABSTRACT

Background: Functional magnetic resonance imaging (fMRI) resting-state studies show generalized social anxiety disorder (gSAD) is associated with disturbances in networks involved in emotion regulation, emotion processing, and perceptual functions, suggesting a network framework is integral to elucidating the pathophysiology of gSAD. However, fMRI does not measure the fast dynamic interconnections of functional networks. Therefore, we examined whole-brain functional connectomics with electroencephalogram (EEG) during resting-state.
Methods: Resting-state EEG data was recorded for 32 patients with gSAD and 32 demographically-matched healthy controls (HC). Sensor-level connectivity analysis was applied on EEG data by using Weighted Phase Lag Index (WPLI) and graph analysis based on WPLI was used to determine clustering coefficient and characteristic path length to estimate local integration and global segregation of networks.
Results: WPLI results showed increased oscillatory midline coherence in the theta frequency band indicating higher connectivity in the gSAD relative to HC group during rest. Additionally, WPLI values positively correlated with state anxiety levels within the gSAD group but not the HC group. Our graph theory based connectomics analysis demonstrated increased clustering coefficient and decreased characteristic path length in theta-based whole brain functional organization in subjects with gSAD compared to HC.
Conclusions: Theta-dependent interconnectivity was associated with state anxiety in gSAD and an increase in information processing efficiency in gSAD (compared to controls). Results may represent enhanced baseline self-focused attention, which is consistent with cognitive models of gSAD and fMRI studies implicating emotion dysregulation and disturbances in task negative networks (e.g., default mode network) in gSAD.

1. Introduction

Generalized social anxiety disorder (gSAD) is a common psychiatric illness characterized by inappropriate fears in a range of situations that involve potential scrutiny by others (Kessler et al., 2005; Stein and Stein, 2008). Cognitive models emphasize preferential processing of internal and external threat signals (e.g., negative thoughts, attentional bias to aversive faces; (Bögels and Mansell, 2004) as key to the development and maintenance of the gSAD (Clark and Wells, 1995; Hope et al., 1989). Accumulating data from task-based functional magnetic resonance imaging (fMRI) studies over the past decade involving negative stimuli indicate such bias is the result of frontolimbic disturbances resulting in limbic/paralimbic hyper-reactivity in emotion processing areas (e.g., amygdala, insula) and aberrant activation (hyper- or hypo-activity) in regions that regulate emotional response (e.g., anterior cingulate cortex, dorsolateral prefrontal cortex) (for review see Brühl et al., 2014).

The neurobiology of gSAD has also been informed with resting-state fMRI studies, which permit examination of intrinsic (spontaneous, task-independent) networks. Various studies have shown anomalous associations between spatially distant regions in gSAD suggesting the disorder involves baseline disruptions in distributed neural systems. For example, there is evidence of decreased frontolimbic functional connectivity and aberrant effective connectivity in gSAD relative to healthy controls (Ding et al., 2011; Hahn et al., 2011; Manning et al., 2015; Prater et al., 2013; Liao et al., 2010; Qiu et al., 2011; Zhang et al., 2015). Similarly, widespread alterations in task positive and negative systems (e.g.,

* Corresponding author at: Department of Psychiatry, University of Illinois at Chicago, 1747 W. Roosevelt Rd, Chicago, IL 60608, United States.
E-mail address: hklumpp@psych.uic.edu (H. Klumpp).
[1] Shared first author.

http://dx.doi.org/10.1016/j.nicl.2016.11.009

dorsal attention network, default mode network, visual network) have been shown in gSAD (Anteraper et al., 2014; Liao et al., 2010; Liu et al., 2015a; Liu et al., 2015b). Taken together, fMRI findings indicate aberrant resting-state activity may underlie a threat-sensitive system in gSAD.

However, inferences of brain organization related to intrinsic activity are limited in fMRI due to its poor temporal resolution. That is, the millisecond to second time scales that reflect considerable information processing at rest are not captured with fMRI. A more appropriate technique is electroencephalogram (EEG), which assesses the fast and lagged spontaneous brain activity in time and frequency enabling the characterization of intrinsic neurocognitive networks (Koenig et al., 2005). Thus far, there has been little application of EEG in the study of gSAD at rest through limited research suggests electrophysiological patterns in gSAD differ from healthy controls. Using traditional power analysis, Sachs et al. (2004) reported a decrease in absolute and relative power in slow frequency bands (i.e., theta and delta) but higher intermediate beta absolute and average power in individuals with gSAD compared to healthy participants (Sachs et al., 2004). Evidence frequency-related vigilance effects (participants were aroused by auditory stimuli if drowsiness was detected) did not diminish at rest suggests gSAD is associated with hyperarousal (Sachs et al., 2004).

To date, there has been no EEG-based resting-state connectivity study in gSAD. Such a study is warranted as abnormal neurophysiological connectivity has been observed in internalizing conditions that share neurobiological features with gSAD (Etkin and Wager, 2007; Hamilton et al., 2015b). For example, individuals with major depressive disorder exhibit higher coherence (e.g., coupling) at rest relative to controls in delta, theta, alpha, and beta frequencies (Leuchter et al., 2012b). Similarly, posttraumatic stress disorder is associated with extensive increased theta and alpha connectivity at rest (Imperatori et al., 2014). Findings are proposed to reflect a loss of selectivity in functional networks, which may underlie symptomatology (e.g., cognitive impairment, emotion dysregulation, memory deficiencies) (Imperatori et al., 2014; Leuchter et al., 2012).

More recently, advances in analytic approaches have enabled the mapping of systems through which the brain is interconnected (i.e., connectomics), thereby increasing our understanding of the topological properties and oscillatory activity in different brain regions and whole-brain functional networks. Therefore, the main aim of the current study was to explore resting-state functional (dys)connectivity in gSAD with Weighted Phase Lag Index (WPLI). WPLI has been shown to circumvent sources of noise that may artificially induce functional connectivity such as volume conduction and reference electrode effects) (Guevara et al., 2005; Nunez et al., 1997) providing a more reliable index of phase synchronization (i.e., phase coupling)(Vinck et al., 2011). Specifically, WPLI measures the distribution of phase angle differences of two channels (i.e., electrodes) across frequency bands in different brain areas. If two channels' functional coupling is strong, the resulting connectivity index will be high in a given frequency domain (Cohen, 2013), which has pathophysiological significance. Phase-coupled activity is an important mechanism in the functional communication between brain regions (Fries, 2005; Gross et al., 2001; Power et al., 2012); thus, an essential aspect of the WPLI is the delineation of reliable estimators to determine the phase relationship between two signals. Given these properties, we applied graph theoretical measures to characterize complex networks (Bullmore, 2012; Bullmore et al., 2009) based on WPLI.

Accordingly, we examined Clustering Coefficient and Characteristic Path Length to identify the local integration and global segregation of networks where information processing efficiency is characterized by high local connectivity along with few long-range connections (Bullmore and Sporns, 2009). Additionally, we explored whether significant WPLI values or indices of global segregation and local integration network results correlated with anxiety measures in gSAD. A secondary aim was to assess whether regionally-based power across different frequency bands differed between individuals with gSAD and healthy controls.

2. Methods

2.1. Participants

All participants provided written informed consent as approved by the local Institutional Review Board at the University of Illinois at Chicago (UIC) and all procedures complied with the Helsinki Declaration. Diagnosis was based on the Structured Clinical Interview for DSM-IV ("SCID-IV"; First et al., 1995) and the clinician-administered Liebowitz Social Anxiety Scale ("LSAS"; Liebowitz, 1987) determined symptom severity. The self-reported Spielberger State-Trait Anxiety Inventory (Spielberger, 1983) and Beck Depression Inventory (Beck et al., 1996) were used to evaluate state anxiety, general anxiety, and depression levels, respectively. Participants were monetarily compensated for their time. Participants were between 18 and 55 years of age, free of major medical or neurologic illness as confirmed by a Board Certified physician. GSAD was required to be the primary diagnosis; however, comorbidity was permitted. All participants were free of psychotropic medications and none was engaged in psychotherapy. Healthy control (HC) participants were required to not have an Axis I disorder. Exclusion criteria for all participants were current substance abuse or dependence (within 6 months of study) or history of major psychiatric illness (e.g., bipolar disorder, psychotic disorder, pervasive developmental disorder).

2.2. EEG task

All participants underwent an 8-minute resting state recording session. Specifically, participants viewed a fixation cross on a blank background and were instructed to try not to think of anything in particular for the duration of the scan. All EEG data were recorded using the Biosemi system (Biosemi, Amsterdam, Netherlands) equipped with an elastic cap with 34 scalp channels.

2.3. EEG data processing

EEG data were preprocessed by the software *Brain Vision Analyzer* (Brain Products, Gilching Germany) and connectivity matrices were generated with the *MATLAB* toolbox *Fieldtrip* (Donders Centre for Cognitive Neuroimaging, Nijmegen, Netherlands). To evaluate phase lag synchronization (i.e., phase coupling) among electrode pairs, resting-state data was segmented into 7 second 'trials.' The minimum number was 15 segments (105 s), which is in the range of other resting-state studies (González et al., 2016; Hardmeier et al., 2014; Yu et al., 2016). All time points and segments were averaged accordingly to standard frequency bands: alpha (8–14 Hz), beta (13–30 Hz), theta (4–8 Hz) and delta (1 Hz–3 Hz).

2.4. Weighted phase lag index

Each index of weighted phased lag is characterized by the distribution of phase angle differences. The instantaneous phase lag and magnitude can be acquired through cross power density spectrums. The cross power density is defined as:

$$S_{xy}(\omega) = \lim_{T\to\infty} \frac{1}{T} E\{Y_x^*(\omega) Y_y(\omega)\} \quad (1)$$

where S_{xy} is the cross spectral density function between signals $y_y(t)$ and $y_x(t)$. $Y_x(\omega)$ in the finite Fourier transform of signal $y_x(t)$ at frequency ω, $Y_x^*(\omega)$ is the complex conjugate of $Y_x(\omega)$, and $E\{\}$ is the expectation. The cross power density is applied within each segment with the frequency of interest (i.e., 1 Hz–50 Hz).

The distribution of phase angle differences can be towards the positive side or the negative side of the complex plane (Cohen, 2013; Vinck et al., 2011). If two signals are uncorrelated, the angular difference will be evenly distributed on the plane, but if two signals are strongly coupled, the difference will be concentrated to one side of the plane demonstrating an asymmetric distribution. The more concentrated the phase angle differences are on the same side, either positive or negative, the higher the phase lag synchronization will be (Cohen, 2013). WPLI is defined as:

$$\mathrm{WPLI}_{xy} = \frac{n^{-1}\sum_{t=1}^{n}|\mathrm{imag}(S_{xyt})|\,sgn(\mathrm{imag}(S_{xyt}))}{n^{-1}\sum_{t=1}^{n}|\mathrm{imag}(S_{xyt})|} \quad (2)$$

where $\mathrm{imag}(S_{xyt})$ indicates the cross-spectral density at time point t in the complex plane xy, and *sgn* is the sign function (−1, +1 or 0).

2.5. Graph theory analysis

Because the unsigned WPLI matrix has values ranging between 0 and 1 (taking the absolute value from the raw WPLI matrix), we used weighted network analyses without thresholding, by setting WPLI values as the edge weights. Two graph measures were computed to evaluate a network's integration and segregation. Quantifying efficiency of information transfer, the characteristic path length (CPL) is the average length of all pairwise shortest paths connecting any node to another (Peters et al., 2013; Stam et al., 2006):

$$\mathrm{CPL} = \frac{1}{|V(G)|(|V(G)|-1)} * \sum_{i\neq j} d(i,j) \quad (3)$$

Here $d(i,j)$ is the shortest graph distance between *nodes* $i,j \in V(G)$, where V is the set containing the vertices of a graph G. By contrast, the weighted clustering coefficient (CC) is the mean nodal CC averaged across all vertices. For any vertex i, its nodal CC measures the degree at which local neighborhood nodes form a cluster and is defined as $C_i = \frac{\sum_j \sum_k w_{ij} w_{jk} w_{ki}}{(\sum_j w_{ij})^2 - \sum_j w_{ij}^2}$, where $j, k \in V(G)$ are immediate neighbors of i, and w_{ij}, w_{jk}, and w_{ik} are corresponding weights (Stam et al., 2006). As the numbers of steps required for the path of two randomly selected nodes in a small-world behaving network increase, the logarithm of the number of nodes N in the network grows proportionally.

Group effects were examined with two-tailed independent *t*-tests. To evaluate relationships between anxiety level and intrinsic activation, we conducted correlations within the gSAD group with significant averaged WPLI results in the Statistical Package for the Social Sciences (Chicago, IL version 22). Non-parametric two-tailed Spearman correlations (Spearman, 1904) were selected due to the non-normal distribution of the data.

2.6. Power analysis

All segmentation parameter and analysis windows are consistent with WPLI and Fast-Fourier transforms were conducted using a Hanning window. Each participant's data were averaged across the epochs for each electrode and the mean absolute power was computed for each of the following frequency bands: alpha (8–14 Hz), beta (13–30 Hz), theta (4–8 Hz) and delta (1 Hz–3 Hz). All EEG power variables and individual electrodes were aggregated to create an average for the 34 channels.

3. Results

3.1. Participants

Thirty-eight patients with gSAD and 36 HC participated in the study. However, 7 participants were removed due to poor signal quality and 3 had too few time points (i.e., <30 s) to conduct analysis. Therefore, the final sample comprised 32 patients with gSAD and 32 demographically-matched HCs. The gSAD group [68.8% (n = 22) female] had a mean ± S.D. age of 26.25 ± 7.14. The HC group had the same gender distribution [68.8% (n = 22) female] ($[\chi^2(1) = 0.00, p = 1.00]$, and there were no differences between the gSAD and HC groups in age [$t(62) = 0.94, p = 0.94$)]. As expected, patients exhibited greater symptom severity indexed by LSAS (gSAD 77.9 ± 16.3; HC 14.7 ± 11.3), trait-anxiety (gSAD 54.5 ± 9.7; HC 25.6 ± 4.8), state-anxiety (gSAD 48.1 ± 11.5; HC 23.6 ± 4.9), and depression levels as measured with BDI (gSAD 17.9 ± 10.1; HC 0.9 ± 1.8) relative to controls (all *p*'s < 0.05).

3.2. EEG functional connectome

WPLI produced a dimensional time-dependent matrix, 34 * 34 * 50 * 130, corresponding to the arrangement of channel * channel * frequency * time. Of note, the first five time points and the last five time points were discarded due to quality control. Time averaged alpha (8–14 Hz), beta (13–30 Hz), theta (4–8 Hz) and delta (1 Hz–3 Hz) wave connectomes in the gSAD group and HC group present the pairwise relation of any two channels within the network. Results showed regional differences in three waves (right column Fig. 1). Alpha had the highest averaged WPLI connectivity across all participants. In theta connectivity, frontal midline channels (e.g., Fz, Cz) showed significantly stronger connections to most electrodes in the gSAD relative to HC group. (See supplement Fig. 1 for theta connectivity for head map).

3.3. Power analyses

Resting-state EEG power was examined with a 2 (Group: gSAD, HC) × 4 (Frequency band: alpha, beta, delta, theta) mixed ANOVA with repeated measures on the last factor. There were no main effects for group or frequency band (all *p*'s > 0.05) and no group x frequency interaction was observed ($p = 0.23$) (Fig. 3).

3.4. Graph theory network measures

The characteristic path length (CPL) of theta connectivity in the HC group was significantly higher than the gSAD group (Fig. 4(A), also in Table 1) and no significant CPL group effects were observed in delta, alpha, or beta connectivity (all *p*'s > 0.05). Regarding clustering coefficient (CC) of theta connectivity, HC exhibited significantly lower CC than gSAD group (Fig. 4(B)) and again delta, alpha, or beta connectivity were not significant (Fig. 4(B)). Together, the theta network demonstrated decreasing global segregation and increasing local integration in the gSAD relative to the HC group.

3.5. EEG connectivity-symptom severity relationship

Analyses were limited to the theta-band frequency due to its observed group effect in WPLI. Within the gSAD group, state anxiety level positively correlated with WPLI in the theta band ($r = 0.31$, $p < 0.04$) and in the same frequency, there was a non-significant trend between trait anxiety level and WPLI ($r = 0.29$, $p = 0.06$) (Fig. 5). No such relationships emerged in the HC group. WPLI values did not correlate with symptom severity in the gSAD group. Additionally, no correlations between trait- and state-anxiety levels and theta-related CC or CPL measures were observed in either group.

4. Discussion

To our knowledge, this is the first study that used EEG-based connectomics and graph theory to examine the oscillatory dynamics of resting state and topological organization of brain connectivity in generalized social anxiety disorder (gSAD). In alpha, the dominate frequency at rest (McEvoy et al., 2000), there was robust connectedness across individuals with gSAD and healthy controls (HC). In addition to alpha, no group effects were detected in beta or delta frequencies. However, in the theta band, we observed a pattern of increased oscillatory frontal midline coherence and higher connectivity in gSAD relative to HC. The gSAD group, relative to the HC group, also exhibited increased clustering coefficient and decreased characteristic path length in the theta connectivity-based brain network suggesting theta-dependent increased information processing efficiency in gSAD. Moreover, within the gSAD group, but not HC group, there was a significant positive correlation between theta connectivity values and state anxiety in addition to a non-significant trend between higher theta values and greater trait anxiety level.

Neuroimaging resting-state studies signify gSAD is associated with alterations in task positive and negative networks (Anteraper et al., 2014; Liao et al., 2010; Liu et al., 2015a; Liu et al., 2015b); however, fMRI cannot measure the fast dynamics of spontaneous oscillatory neural activity in frequency ranges associated with large-scale cortical networks (Hipp et al., 2012) due to its slow time resolution. EEG permits evaluation of 'communication-through-coherence', where the synchronization of oscillatory activity is believed to reflect effective communication structures (Fries, 2005). Namely, coherence changes are an indicator of information flow along local and/or distant interconnecting pathways (Petsche, 1996). Multiple methods have been established to calculate EEG connectivity, including power correlation and causality based methods. Here, we used a Weighted Phase Lag Index (WPLI), a commonly used method for data-driven and exploratory analyses (Cohen, 2013) known for its sensitivity in detecting phase-

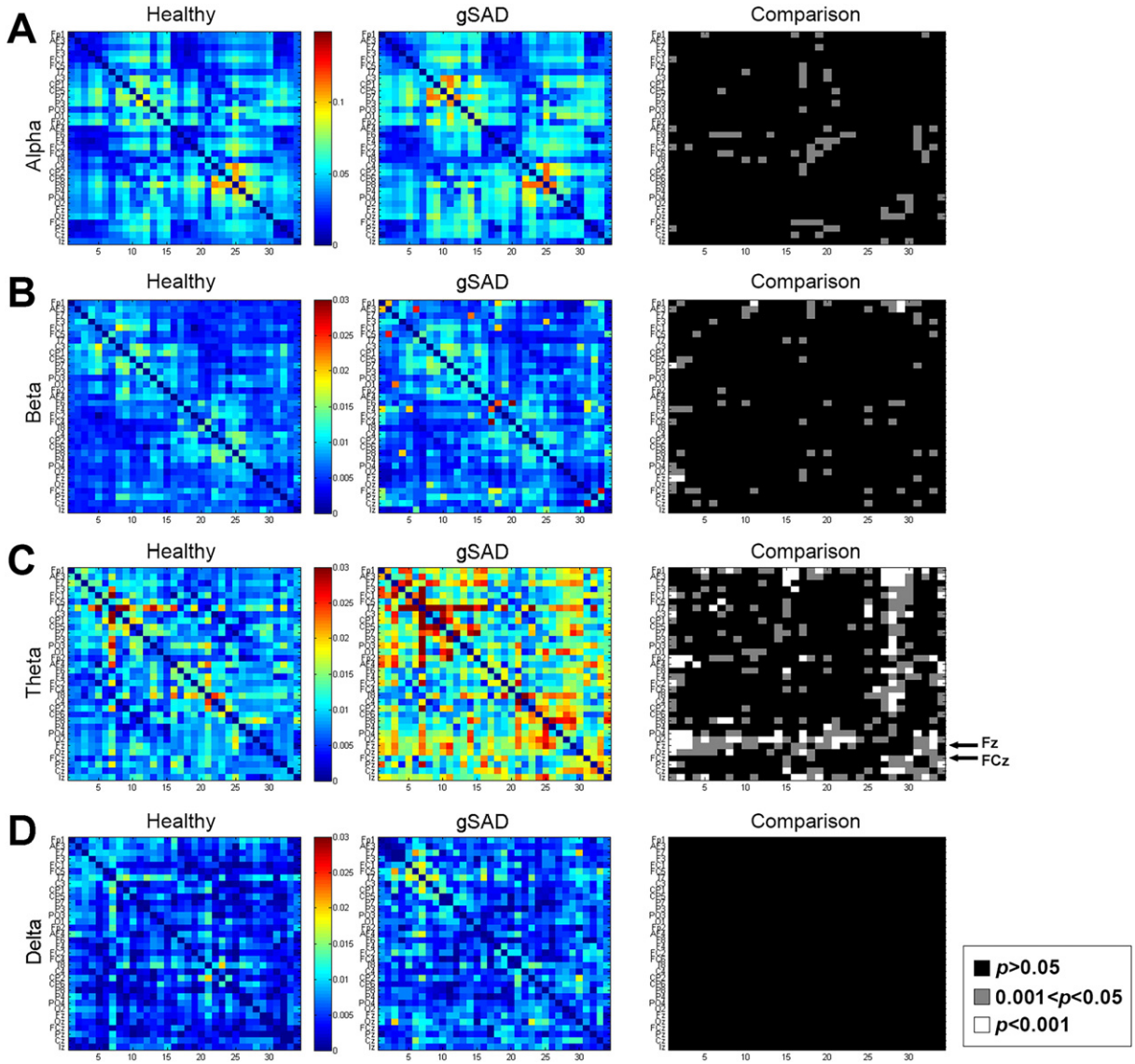

Fig. 1. WPLI connectivity during resting state in the healthy group (left column) and the gSAD group (middle column). WPLI mapping of three frequency waves: Alpha (first row), Beta (second row), Theta (third row) and Beta (forth row) were generated from the averaged 32 participants with gSAD and 32 controls. Paired *t*-tests were applied to every region across two groups; regions with $0.001 < p < 0.05$ were marked in gray (third column), regions with $p < 0.001$ were marked in white. Channels 1 to 14 were located in the left hemisphere, 15–18 in the right hemisphere and 29–34 midline channels. Theta connectivity shows the midline frontal channel (Fz and FCz) is significantly higher in gSAD relative to healthy controls (marked with arrows.)

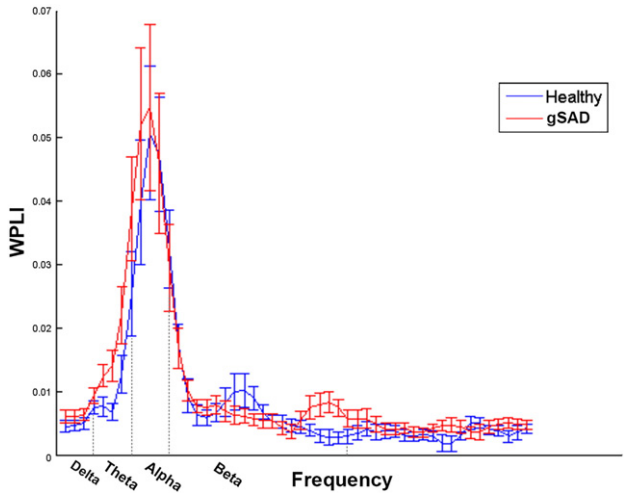

Fig. 2. Variation of averaged WPLI with the frequency in healthy and gSAD group. Additionally, group effects were observed in the theta frequency band where the gSAD group had significantly higher WPLI values compared to the HC group. (Fig. 2).

synchronization (Vinck et al., 2011). WPLI was used to examine oscillatory synchronization of resting-state in frequency bands previously reported to be disturbed in internalizing psychopathologies (e.g., alpha, theta, beta, delta) (Imperatori et al., 2014; Leuchter et al., 2012b; Sachs et al., 2004) and graph analysis was employed to describe network properties.

Group differences were observed in the theta frequency band. Evidence of alterations in resting-state theta band regional power have been reported in gSAD studies (Gerez et al., 2016; Sachs et al., 2004) and anomalous theta power or network connectivity has been shown in other disorders like depression (Leuchter et al., 2012b), obsessive-compulsive disorder (Koprivova et al., 2011), and post-traumatic stress disorder (Imperatori et al., 2014). Thus, our results are in line with above-mentioned reports of theta oscillation involvement internalizing conditions.

Notably, we observed increased frontal midline theta connectivity in gSAD compared to controls. Resting-state frontal midline theta rhythm, generated by regions implicated in the anterior attentional system (e.g., anterior cingulate cortex) (Asada et al., 1999), is associated with mental task performance and meditative concentration reflecting focused attentional processing in healthy participants (Inanaga, 1998; Kubota et al., 2001). Moreover, frontal theta EEG activity is considered an index of the default mode network (DMN) (Scheeringa et al., 2008), a task-negative cognitive network implicated in self-referential processes and emotion regulation (Raichle et al., 2001; Shulman et al., 1997). In the gSAD group, greater frontal theta values corresponded with higher levels of state- and trait-anxiety levels though the trait anxiety finding was at a non-significant trend. No correlations in gSAD were detected for symptom severity as assessed with the LSAS, which evaluates fear and avoidance levels in various social situations (Liebowitz, 1987). Of note, the significant relationship between frontal theta and state anxiety was not observed in the HC group.

In gSAD, the link between theta-related connectivity and state anxiety indicate more internalized attention (e.g., negative self-focused thoughts, emotions, and/or general rumination) (Hamilton et al., 2015a) when engaged in task-independent thought (i.e., mind-wandering). Neuroimaging studies of gSAD have reported abnormal functional connectivity in the DMN (Gentili et al., 2009; Liao et al., 2010). Also, multivariate classification shows regions integral to DMN, in addition to other systems (e.g., perceptual networks), significantly discriminate individuals with gSAD from HC. It is proposed that activity reflecting DMN engagement in social anxiety may be related to attention to negative thoughts and feelings such that self-focused attention to internally generated information contributes to the distorted impressions that characterize gSAD (Clark and Wells, 1995; Gentili et al., 2009). More broadly, a meta-analytic study of task-based frontal midline theta (~4–8 Hz oscillations recorded from sensors on the scalp overlying midcingulate cortex; 'MCC') revealed theta signals reflecting MCC activity integral to cognitive control is disturbed in anxious individuals (Cavanagh and Shackman, 2015). Our resting-state findings suggest intrinsic tonic abnormalities may underlie a threat-sensitive system in gSAD due in part to the disturbances in controlled processes that regulate emotions (Brühl et al., 2014).

Recently, graph theory has shown the brain structural or functional organization can be examined from the perspective of a "small-world" characteristic. Small-worldness mainly encompasses dominant local but infrequent long-range connections expressed by connectomics measures of high clustering coefficient (the degree that the nodes in a graph tend to cluster together) and lower characteristic path length (average of shortest paths from each node to another one in a graph); both of these features reflect information processing efficiency at a low cost (Bullmore and Sporns, 2009; Rubinov and Sporns, 2010). Here, we observed changes in connectomics metrics of whole brain network theta connectivity in which small-worldness in theta-band frequency was enhanced (increase in clustering coefficient and decrease in characteristic path length) in gSAD subjects compared to HC pointing to a more efficient theta network in gSAD. However, indices of worldness were not associated with anxiety level or symptom severity in gSAD.

We propose the stronger resting-state theta network activity in gSAD is related to pathologic dynamics for the following reasons. First, theta oscillations in general is not a dominant resting-state activity

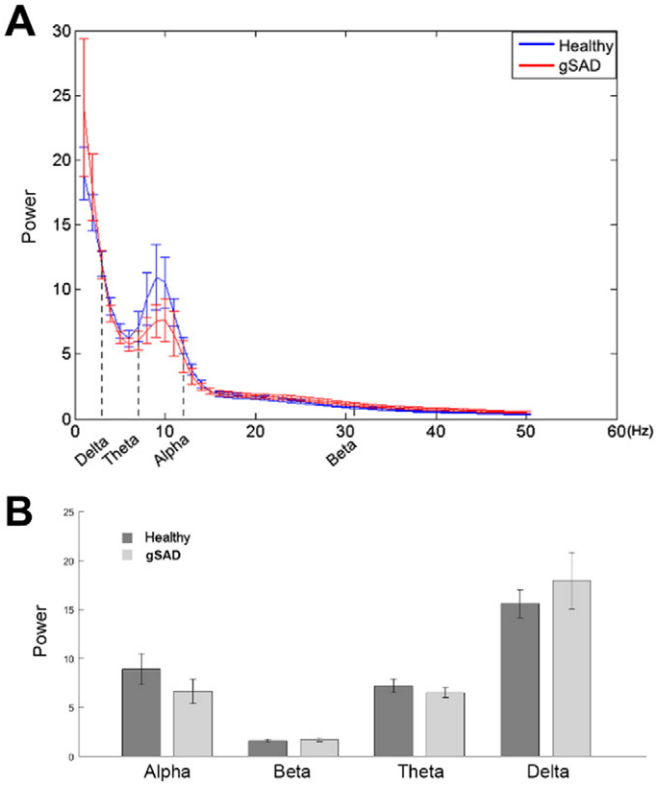

Fig. 3. (A) Power variation from 1 Hz–50 Hz; (B) averaged power of alpha, beta, theta and delta.

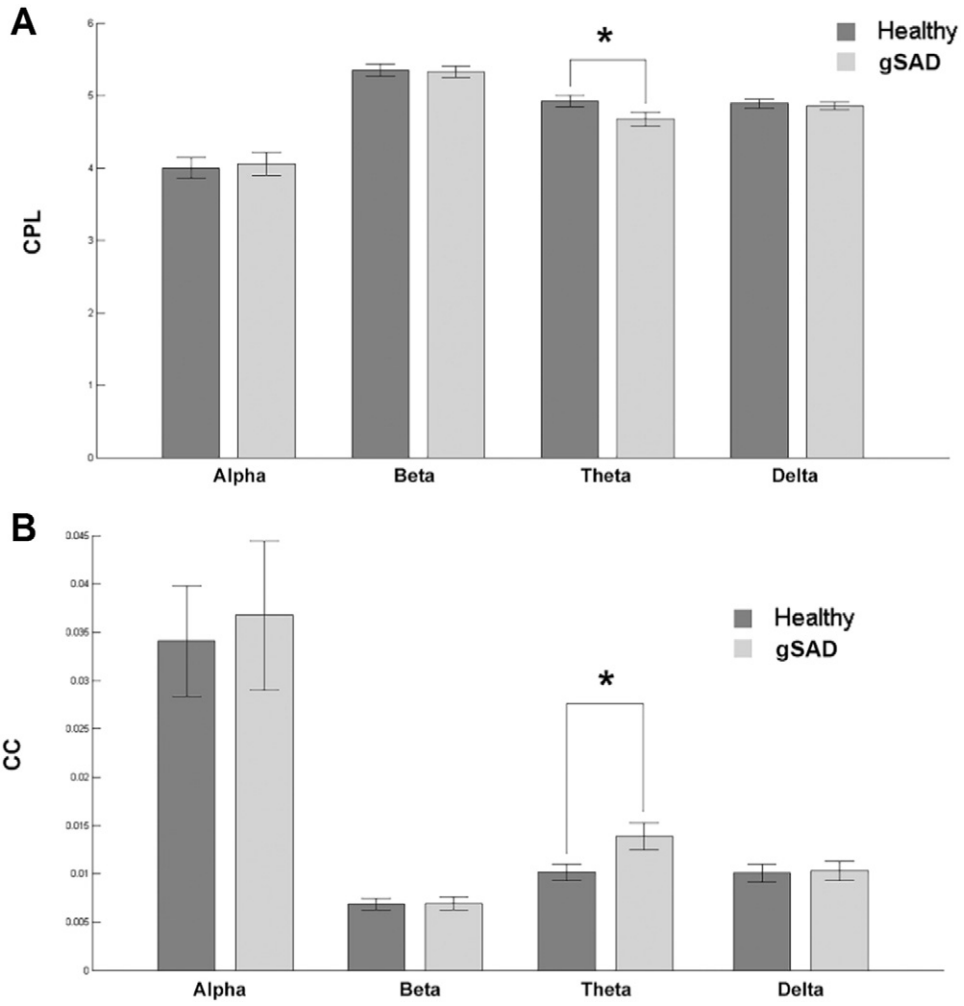

Fig. 4. (A) Characteristics path length of alpha, beta, theta and delta wave in the healthy control and gSAD groups. (B) Clustering coefficient of alpha, beta and theta in the two groups.

and, as noted above, an increase in theta power and connectivity (measured by different methods) has been shown to be associated with abnormality in affective disorders such as depression, obsessive compulsive disorder, and posttraumatic stress disorder (Imperatori et al., 2014; Koprivova et al., 2011; Leuchter et al., 2012b). Second, our connectivity results and its association with state anxiety suggest theta activity in gSAD represents an increased state of internalized attention (e.g., attention to negative thoughts or emotions). Consequently, the theta-dependent small-worldness may reflect increased efficiency in an inter-modal functional network associated with rumination or other maladaptive self-referential propensities. Nevertheless, taking into consideration neuroimaging findings of extensive abnormalities in task positive and negative systems (Anteraper et al., 2014; Liao et al., 2010; Liu et al., 2015a; Liu et al., 2015b), it is possible that theta-band connectivity represents cognitive processes beyond DMN.

Considering the significant connectivity and connectomics findings and lack of group effects with power analysis, network analysis with WIPLI and connectomics may be more sensitive in detecting aberrant neurophysiological resting-state connectivity in gSAD than more traditional regionally-based power analysis.

Findings should be interpreted in the context of important limitations. First, we used a sensor-based approach in our connectivity analyses. This approach does not allow us to define the exact anatomical sources of EEG signals. High resolution EEG recording combined with source localization methods can provide better spatial resolution in EEG-based connectivity analysis. Second, the experimental design is cross-sectional, thus, it is not clear whether findings change over time. Third, results are based on a gSAD cohort and may not generalize to other anxiety disorders or internalizing conditions. Fourth, our sample size was moderate and failure to detect an association between connectomic results and social anxiety symptoms may have been due to lack of power. Fifth, although WPLI is less sensitive to sources of noise (e.g. heartbeat) than other approaches (e.g., phase lagged index) (Vinck et al., 2011), we cannot rule out possible influences of noise in findings.

In conclusion, a major contribution of the current study is the integrated use of the WPLI and graph theoretical measures to describe the local integration and global segregation of networks in gSAD relative to HC. It was demonstrated that whole brain resting-state theta-based connectomics was altered in gSAD such that theta midfrontal connectivity was higher in the gSAD than HC group and positively associated with state anxiety level in gSAD. We also observed enhanced 'small worldness' in WPLI theta-dependent connectivity in gSAD compared to HC. Taken together, preliminary findings suggest resting-state brain oscillations in gSAD may reflect self-focused negative internal processing, which is consistent with cognitive models of social anxiety disorder (Clark and Wells, 1995). Further study is required to evaluate whether

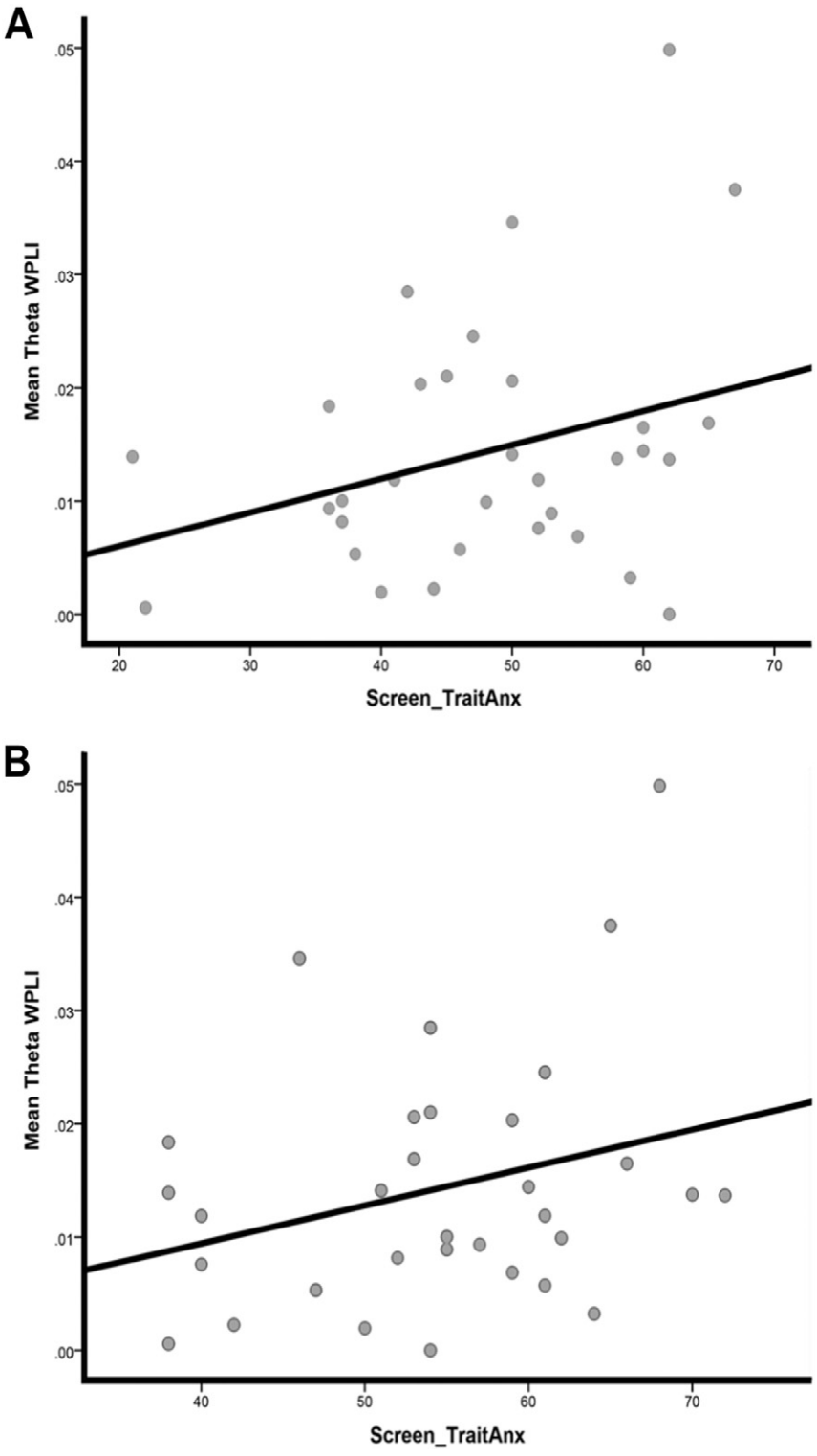

Fig. 5. Trait anxiety scores (A) and state anxiety scores (B) for gSAD subjects.

network connectivity in the theta frequency band is a stable neurophysiological biomarker of gSAD.

Financial disclosure

Ms. Xing and Drs. Tadayonnejad, MacNamara, Ajilore, DiGangi, Phan, Leow, and Klumpp report no competing interests.

Acknowledgements

This work was supported by NIMH K23MH093679 (HK) and in part by NIMH R01MH101497 (KLP) and the Center for Clinical and Translational Research (CCTS) UL1RR029879, and University of Illinois at Chicago Campus Research Board Award.

Table 1
Graph measures for each frequency waves in HC and gSAD. Only theta shows significant difference in CPL and CC (two sample t-test $p < 0.05$).

		Delta	Theta	Alpha	Beta
CC	HC	0.010 ± 0.005	0.010 ± 0.001	0.034 ± 0.005	0.007 ± 0.001
	gSAD	0.010 ± 0.006	0.014 ± 0.001	0.034 ± 0.004	0.007 ± 0.001
	p	0.437	0.013*	0.0392	0.470
CPL	HC	4.890 ± 0.063	4.922 ± 0.075	4.000 ± 0.140	5.347 ± 0.085
	gSAD	4.857 ± 0.057	4.674 ± 0.094	4.051 ± 0.157	5.322 ± 0.079
	p	0.355	0.023*	0.403	0.414

Appendix A. Supplementary data

Supplementary data to this article can be found online at http://dx.doi.org/10.1016/j.nicl.2016.11.009.

References

Anteraper, A., Triantafyllou, C., Sawyer, A., Hofmann, S., Gabrieli, J., Whitfield-Gabrieli, S., 2014. Hyper-connectivity of subcortical resting-state networks in social anxiety disorder. Brain Connect. 4 (2), 81–91.

Asada, H., Fukuda, Y., Tsunoda, S., Yamaguchi, M., Tonoike, M., 1999. Frontal midline theta rhythms reflect alternative activation of prefrontal cortex and anterior cingulate cortex in humans. Neurosci. Lett. 274 (1), 29–33.

Beck, A.T., Steer, R.A., Brown, G., 1996. Manual for the Beck Depression Inventory-II. Psychological Corporation, San Antonio, TX.

Bögels, S.M., Mansell, W., 2004. Attention processes in the maintenance and treatment of social phobia: hypervigilance, avoidance and self-focused attention. Clin. Psychol. Rev. 24 (7), 847–877.

Brühl, A.B., Delsignore, A., Komossa, K., Steffi, W., 2014. Neuroimaging in social anxiery disorder—a meta-analytic review in a new neurofunctional model. Neurosci. Biobehav. Rev. 47, 260–280.

Bullmore, E., 2012. Functional network endophenotypes of psychotic disorders. Biol. Psychiatry 71 (10), 844–846.

Bullmore, E., Sporns, O., 2009. Complex brain networks: graph theoretical analysis of structural and functional systems. Nat. Rev. Neurosci. 10, 186–199.

Bullmore, E., Barnes, A., Bassett, D.S., Fornito, A., Kitzbichlera, M., Meunier, D., Suckling, J., 2009. Generic aspects of complexity in brain imaging data and other biological systems. NeuroImage 47 (3), 1125–1135.

Cavanagh, J.F., Shackman, A.J., 2015. Frontal midline theta reflects anxiety and cognitive control: meta-analytic evidence. J. Physiol. Paris 109, 3–16.

Clark, D.M., Wells, A., 1995. A cognitive model of social phobia. In: Heimberg, R.G., Liebowitz, M.R., Hope, D.A., Schneier, F.R. (Eds.), Social Phobia: Diagnosis, Assessment, and Treatment. Guilford Press, New York, pp. 69–93.

Cohen, M.X., 2013. Analyzing Neural Time Series Data: Theory and Practice. The MIT Press, London.

Ding, J., Chen, H., Qiu, C., Liao, W., Warwick, J., Duan, X., Zhang, W., Gong, Q., 2011. Disrupted functional connecticity in social anxiety disorder: a resting-state fMRI study. Magn. Reson. Imaging 29, 701–711.

Etkin, A., Wager, T.D., 2007. Functional neuroimaging of anxiety: a meta-analysis of emotional processing in PTSD, social anxiety disorder, and specific phobia. Am. J. Psychiatr. 164 (10), 1476–1489.

First, M., Spitzer, R., Gibbon, M., Williams, J., 1995. Structured Clinical Interview for DSM-IV Axis I Disorders, Patient Edition (SCID-P) (Biometrics Research).

Fries, P., 2005. A mechanism for cognitive dynamics: neuronal communication through neuronal coherence. Trends Cogn. Sci. 9 (10), 474–481.

Gentili, C., Ricciardi, E., Gobbini, M.I., Santarelli, M.F., Haxby, J.V., Pietrini, P., Guazzelli, M., 2009. Beyond amygdala: default mode network activity differs between patients with social phobia and healthy controls. Neuroscience 79 (6), 13–409.

Gerez, M., Suarez, E., Serrano, C., Castanedo, L., Tello, A., 2016. The crossroads of anxiety: distinct neurophysiological maps for different symptomatic groups. Neuropsychiatr. Dis. Treat. 12, 75–159.

González, G.F., Molen, M.J.W.V.d., Žarić, G., M.B., Tijms, J., Blomert, L., Stam, C.J., Molen, M.W.V.d., 2016. Graph analysis of EEG resting state functional networks in dyslexic readers. Clin. Neurophysiol. 127, 3165–3175.

Gross, J., Kujala, J., Hamalainen, M., Timmermann, L., Schnitzler, A., Salmelin, R., 2001. Dynamic imaging of coherent sources: studying neural interactions in the human brain. PNAS 98 (2), 686–688.

Guevara, R., Velazquez, J.L.P., Nenadovic, V., Wennberg, R., Senjanovic, G., Dominguez, L.G., 2005. Phase synchronization measurements using electroencephalographic recordings what can we really say about neuronal synchrony? Neuroinformatics 3, 301–313.

Hahn, A., Stein, P., Windischberger, C., Weissenbacher, A., Spindelegger, C., Moser, E., Kasper, S., Lanzenberger, R., 2011. Reduced resting-state functional connectivity between amygdala and orbitofrontal cortex in social anxiety disorder. NeuroImage: Clinical 56 (3), 811–820.

Hamilton, J.P., Farmer, M., Fogelman, P., Gotlib, I.H., 2015. Depressive rumination, the default-mode network, and the dark matter of clinical neuroscience. Biol. Psychiatry 78 (4), 30–224.

Hardmeier, M., Hatz, F., Bousleiman, H., Schindler, C., Stam, C.J., Fuhr, P., 2014. Reproducibility of functional connectivity and graph measures based on the Phase Lag Index (PLI) and Weighted Phase Lag Index (wPLI) derived from high resolution EEG. PLoS One 9.

Hipp, J.F., Hawellek, D.J., Corbetta, M., Siegel, M., Engel, A.K., 2012. Large-scale cortical correlation structure of spontaneous oscillatory activity. Nat. Neurosci. 15, 844–851.

Hope, D.A., Gansler, D.A., Heimberg, R.G., 1989. Attentional focus and causal attributions in social phobia: implications from social psychology. Clin. Psychol. Rev. 9 (1), 49–61.

Imperatori, C., Farina, B., Quintiliani, M.I., Onofri, A., Castelli Gattinara, P., Lepore, M., Gnoni, V., Mazzucchi, E., Contardi, A., Della Marca, G., 2014. Aberrant EEG functional connectivity and EEG power spectra in resting state post-traumatic stress disorder: a sLORETA study. Biol. Psychol. 102, 7–10.

Inanaga, K., 1998. Frontal midline theta rhythm and mental activity. Psychiatry Clin. Neurosci. 52 (6), 555–567.

Kessler, R.C., Berglund, P., Demler, O., Jin, R., Merikangas, K.R., EE., W., 2005. Lifetime prevalence and age-of-onset distributions of DSM-IV disorders in the National Comorbidity Survey Replication. Arch. Gen. Psychiatry 62 (6), 593–603.

Koenig, T., Studer, D., Hubl, D., Melie, L., Strik, W., 2005. Brain connectivity at different time-scales measured with EEG. Philos. Trans. R. Soc. B 360 (1457), 1015–1025.

Koprivova, J., Congedo, M., Horacek, J., Prasko, J., Raszka, M., Brunovsky, M., Kohutova, B., Hoschl, C., 2011. EEG source analysis in obsessive-compulsive disorder. Clin. Neurophysiol. 122 (9), 43–1735.

Kubota, Y., Sato, W., Toichi, M., Murai, T., Okada, T., Hayashi, A., Sengoku, A., 2001. Frontal midline theta rhythm is correlated with cardiac autonomic activities during the performance of an attention demanding meditation procedure. Cogn. Brain Res. 11 (2), 281–289.

Leuchter, A.F., Cook, I.A., Hunter, A.M., Cai, C., Horvath, S., 2012. Resting-state quantitative electroencephalography reveals increased neurophysiologic connectivity in depression. PLoS One 7, e32508.

Liao, W., Chen, H., Feng, Y., Mantini, D., Gentili, C., Pan, Z., Ding, J., Duan, X., Qiu, C., Lui, S., Gong, Q., Zhang, W., 2010. Selective aberrant functional connectivity of resting state networks in social anxiety disorder. NeuroImage 52 (4), 1549–1559.

Liebowitz, M., 1987. Liebowitz social anxiety scale. Social phobia. Mod. Probl. Pharmacopsychiatry 22, 414–447.

Liu, F., Guo, W., Fouche, J.-P., Wang, Y., Wang, W., Ding, U., Zeng, L., Qiu, C., Gong, Q., Zhang, W., Chen, H., 2015a. Multivariate classification of social anxiety disorder using whole brain functional connectivity. Brain Struct. Funct. 220, 101–116.

Liu, F., Zhu, C., Wang, Y., Guo, W., Li, M., Wang, W., Long, Z., Meng, Y., Cui, Q., Zeng, L., Gong, Q., Zhang, W., Chen, H., 2015b. Disrupted cortical hubs in functional brain networks in social anxiety disorde. Clin. Neurophysiol. 126, 1717–1732.

Manning, J., Reynolds, G., Saygin, Z.M., Hofmann, S.G., Pollack, M., Gabrieli, J.D.E., Whitfield-Gabrieli, S., 2015. Altered resting-state functional connectivity of the frontal-striatal reward system in social anxiety disorder. PLoS One 1–15.

McEvoy, L.K., Smith, M.E., Gevins, A., 2000. Test–retest reliability of cognitive EEG. Clin. Neurophysiol. 111 (3), 457–464.

Nunez, P., Srinivasan, R., Westdorp, A., Wijesinghe, R., Tucker, D., Silberstein, R., Cadusch, P., 1997. EEG coherency I: statistics, reference electrode, volume conduction, Laplacians, cortical imaging, and interpretation at multiple scales. Electroencephalogr. Clin. Neurophysiol. 103, 499–515.

Peters, J.M., Taquet, M., Vega, C., Jeste, S.S., Fernández, I.S., Tan, J., Nelson, C.A., Sahin, M., Warfield, S.K., 2013. Brain functional networks in syndromic and non-syndromic autism: a graph theoretical study of EEG connectivity. BMC Med. 11 (1), 1–16.

Petsche, H., 1996. Approaches to verbal, visual and musical creativity by EEG coherence analysis. Int. J. Psychophysiol. 24 (1–2), 59–146.

Power, J.D., Barnes, K.A., Snyder, A.Z., Schlaggar, B.L., Petersen, S.E., 2012. Spurious but systematic correlations in functional connectivity MRI networks arise from subject motion. NeuroImage 59 (3), 2154–2163.

Prater, K., Hosanagar, A., Klumpp, H., Angstadt, M., Phan, K.L., 2013. Aberrant amygdala-frontal cortex connectivity during perception of fearful faces and at rest in generalized social anxiety disorder. Depress. Anxiety 30 (3), 234–242.

Qiu, C., Liao, W., Ding, J., Feng, Y., Zhu, C., Nie, X., Wei Zhang, W., Chen, H., Gong, Q., 2011. Regional homogeneity changes in social anxiety disorder: a resting-state fMRI study. Psychiatry Res. Neuroimaging 194, 47–53.

Raichle, M.E., MacLeod, A.M., Snyder, A.Z., Powers, W.J., Gusnard, D.A., Shulman, G.L., 2001. A default mode of brain function. NeuroImage 98 (2), 1083–1091.

Rubinov, M., Sporns, O., 2010. Complex network measures of brain connectivity: uses and interpretations. NeuroImage 52 (3), 69–1059.

Sachs, G., Anderer, P., Dantendorfer, K., Saletu, B., 2004. EEG mapping in patients with social phobia. Psychiatry Res. 131 (3), 47–237.

Scheeringa, R., Bastiaansen, M.C.M., Petersson, K.M., Oostenveld, R., Norris, D.G., Hagoort, P., 2008. Frontal theta EEG activity correlates negatively with the default mode network in resting state. Int. J. Psychophysiol. 67 (3), 242–252.

Shulman, G.L., Fiez, J.A., Corbetta, M., Buckner, R.L., Miezin, F.M., Raichle, M.E., Petersen, S.E., 1997. Common blood flow changes across visual tasks: II. Decreases in cerebral cortex. J. Cogn. Neurosci. 9 (5), 648–664.

Spearman, 1904. The proof and measurement of association between two things. Am. J. Psychol. 15, 72–102.

Spielberger, C., 1983. Manual for the State-Trait Anxiety Inventory (form Y). Consulting Psychologists Press.
Stam, C., Jones, B., Nolte, G., Breakspear, M., Scheltens, P., 2006. Small-world networks and functional connectivity in Alzheimer's disease. Cereb. Cortex 17 (1), 92–100.
Stein, M.B., Stein, D.J., 2008. Social anxiety disorder. Lancet 371 (9618), 1115–1126.
Vinck, M., Oostenveld, R., Wingerden, M.v., Battaglia, F., Pennartz, C.M.A., 2011. An improved index of phase-synchronization for electrophysiological data in the presence of volume-conduction, noise and sample-size bias. NeuroImage 55 (4), 1548–1566.
Yu, M., Gouw, A.A., Hillebrand, A., Tijms, B.M., Stam, C.J., Straaten, E.C.W.v., Pijnenburg, Y.A.L., 2016. Different functional connectivity and network topology in behavioral variant of frontotemporal dementia and Alzheimer's disease: an EEG study. Neurobiol. Aging 42, 150–162.
Zhang, Y., Zhu, C., Chen, H., Duan, X., Lu, F., Li, M., Liu, F., Ma, X., Wang, Y., Zeng, L., Zhang, W., Chen, H., 2015. Frequency-dependent alterations in the amplitude of low-frequency fluctuations in social anxiety disorder. 174 pp. 329–335.